Photoresponse of ^{76}Se below 9 MeV

N. Cooper,[1] F. Reichel,[2] V. Werner,[1] L. Bettermann,[1,3] B. Alikhani,[2] S. Aslanidou,[2] C. Bauer,[2] L. Coquard,[2] M. Fritzsche,[2] Y. Fritzsche,[2] J. Glorius,[2] P. M. Goddard,[1,4] T. Möller,[2] N. Pietralla,[2] M. Reese,[2] C. Romig,[2] D. Savran,[5,6] L. Schnorrenberger,[2] F. Siebenhühner,[2] V. V. Simon,[7,8] K. Sonnabend,[2,9] M. K. Smith,[1] C. Walz,[2] S. W. Yates,[10] O. Yevetska,[2] and M. Zweidinger[2]

[1]*Wright Nuclear Structure Laboratory, Yale University, New Haven, Connecticut 06520-8120, USA*

[2]*Institut für Kernphysik, Technische Universität Darmstadt, 64289 Darmstadt, Germany*

[3]*Institut für Kernphysik, Universität zu Köln, 50937 Köln, Germany*

[4]*Department of Physics, University of Surrey, Guildford, GU2 7XH, United Kingdom*

[5]*ExtreMe Matter Institute and Research Devision, GSI, Planckstr. 1, 64291 Darmstadt, Germany*

[6]*Frankfurt Institute for Advanced Studies, Ruth-Moufang-Str. 1, 60438 Frankfurt, Germany*

[7]*Fakultät für Physik und Astronomie, Ruprecht-Karls-Universitaet Heidelberg, 69120 Heidelberg, Germany*

[8]*TRIUMF, 4004 Wesbrook Mall, Vancouver, British Columbia, V6T 2A3 Canada*

[9]*Goethe Universität Frankfurt, 60438 Frankfurt am Main, Germany*

[10]*Departments of Chemistry and Physics & Astronomy, University of Kentucky, Lexington, Kentucky, 40506-0055, USA*

(Received 15 June 2012; published 10 September 2012)

The dipole strength distribution of ^{76}Se has been investigated via photon scattering in the energy region below 9 MeV utilizing bremsstrahlung produced at the S-DALINAC facility at the TU Darmstadt. About 0.20(1)% of the classical $E1$ sum rule is exhausted by observed $J = 1$ states of justifiably assumed negative parity. An extrapolation of the GDR below 9 MeV suggests that considerable strength may remain unobserved due to background, finite detector resolution, and fragmentation. The observed strength thus represents a lower limit. Candidates for the $2^+_{1,\mathrm{ms}}$ state and a fragment of the 1^+_{sc} mixed-symmetry states are presented.

DOI: 10.1103/PhysRevC.86.034313 PACS number(s): 25.20.Dc, 24.30.Cz, 27.50.+e

I. INTRODUCTION

There has been recent interest in the dipole strength of nuclei near the neutron separation energy. Earlier works reported enhancements of dipole strength at low energy in ^{140}Ce and ^{138}Ba [1,2], and the term *pygmy dipole resonance* (PDR) was used to describe the phenomenon. The states observed in ^{138}Ba were soon unambiguously assigned $J^\pi = 1^-$ through polarized photon-scattering experiments [3]. Many subsequent studies, primarily in closed-shell nuclei, reported similar results (e.g., Refs. [4–12]). One possible explanation of excess electric dipole strength include a core-skin vibration [13–15], an idea inspired in part by the observation of a neutron skin in light neutron-rich nuclei [16] and the enhanced $E1$ strength seen in very neutron-rich exotic nuclei [17,18]. Other possibilities include octupole deformations and α clustering as proposed by Iachello [19].

Of specific interest for ^{76}Se is its location at or beyond the onset of deformation, with a quadrupole deformation of $\beta = 0.31$. Much attention has been paid experimentally to spherical nuclei in the study of the PDR and, in particular, the dependence of excitation strength on neutron excess or neutron skin thickness. If the core-skin vibration is an accurate picture of the PDR, one would expect that in axially symmetric, quadrupole-deformed nuclei the resonance splits into two energy-separated resonances, each corresponding to a vibration either parallel or perpendicular to the symmetry axis.

Another interest in ^{76}Se comes from the hypothetical neutrinoless double β-decay ($0\nu2\beta$-decay) mode of ^{76}Ge. If the neutrino is a Majorana particle, i.e., its own antiparticle [20], the $0\nu2\beta$-decay mode would be possible and the sum energy of coincident electrons observed from double β decay should display a peak near the Q value [21]. Klapdor-Kleingrothaus *et al.*, in the Heidelberg-Moscow experiment, claimed a first $0\nu2\beta$-decay observation in ^{76}Ge [22]. Confirmation of this result is currently being sought in, e.g., the GERDA [23] and MAJORANA [24] experiments. If the claimed observation is correct, the decay width of this mode would allow calculation of the neutrino mass if the nuclear matrix elements were known. Much effort has been put into the calculation of the matrix elements in various models, including the shell model, quasiparticle random-phase approximation (QRPA), and the interacting boson model 2 (IBM-2) (see, e.g., Refs. [25–28]). The matrix elements obtained from the different models exhibit considerable disagreement. Consequently, experimental data to pinpoint the structure of nuclei in the region of $0\nu2\beta$-decay candidates is desirable in order to help constrain the model calculations. Resonance strengths, such as that of the PDR, have been previously described by the QRPA. Related experimental data may help constrain the matrix element calculations in theories sensitive to dipole strength distributions.

The quadrupole-octupole coupled (QOC) 1^- vibrational state is another $E1$ excited collective state which lies at low energy. The state is one of five states which may be formed by coupling a quadrupole vibrational phonon to an octupole vibrational phonon. In a harmonic coupling scheme, the QOC 1^- state lies near the sum energy of the 2^+_1 and 3^-_1 states. In addition to the geometric picture, QOC states have also been addressed in the IBM framework (e.g., Refs. [29,30]). The 1^- QOC state has been well studied in spherical, heavy nuclei. An overview of these studies may be found in Ref. [31].

Although the ground-state quadrupole deformation of ^{76}Se is fairly large, the low-lying excitations still closely resemble a vibrational structure. The $R_{4/2} \equiv E(4_1^+)/E(2_1^+)$ is often used to infer structure of low-lying excitations in nuclei. An $R_{4/2} < 2$ indicates the nucleus is magic, while values near 2 and 3.33 indicate a spherical vibrator and deformed rotor, respectively. For ^{76}Se, $R_{4/2} = 2.38$, which indicates more vibrational than rotational structure. This fact is reconciled with the relatively large ground-state deformation by recognizing that rotational state energies are inversely proportional to the moment of inertia, the latter of which drops rapidly with decreasing A. The interpretation of low-lying states in ^{76}Se as vibrational thus allows one to interpret the structure of negative parity states with $1 < J < 5$ near the sum energy $E(2_1^+) + E(3_1^-)$ to be possible QOC vibrations.

Among positive-parity states that are expected at low energies are the so-called mixed-symmetry (MS) states. These states occur due to the proton-neutron degree of freedom, and differ from fully symmetric (FS) states in that they are nonsymmetric under the exchange of proton and neutron labels in their wave functions. In near-spherical nuclei, the lowest MS state is a 2^+ state, excited from the ground state by an isovector $E2$ transition [32,33]. Analogously to the FS 2_1^+ state, the MS 2_1^+ state is connected to the ground state by a one-phonon MS excitation; however, the $E2$ matrix element of the MS excitation is considerably weaker. States with the properties of the first MS 2^+ and higher-lying MS states were first identified just over a decade ago in ^{94}Mo [34,35].

In a phonon scheme, the FS and MS 2^+ states can be coupled to form a multiplet with $J^\pi = 0^+, \ldots, 4^+$, which would have MS character as well. This can be quantified by the F-spin quantum number, defined within the framework of the interacting boson model (IBM-2) [36,37]. F-spin is the bosonic analog to isospin. FS states have maximum F-spin of $F_{\max} = N/2$, where N is the total number of valence bosons, whereas the MS states considered here are characterized by $F = F_{\max} - 1$. An extensive review on the topic can be found in Ref. [38]. In well-deformed nuclei, the 1^+ member of the two-phonon MS multiplet evolves into the well-known scissors mode [36,39–42], which in a geometrical interpretation is a scissors like counter oscillation of the deformed proton and neutron bodies. It is usually found between about 2.7 and 4 MeV [43,44] and is the band head of a $K = 1$ rotational band. Also in well-deformed nuclei, the scissors mode decays by a strongly collective $M1$ transition to the ground state, whereas this decay is suppressed in near-spherical nuclei due to phonon selection rules. Hence, the excitation strength of the scissors mode, which can be selectively excited in photon scattering, is sensitive to the structure and deformation of the nucleus. The one-phonon MS 2^+ state is expected to fragment toward the rotational limit, one fragment of which should become a member of the MS $K = 1$ band. This transition, however, has not been observed to date, since data on 2^+_{MS} states at the onset of deformation is sparse due to the experimental difficulties in populating these states and in determining their lifetimes and decay properties.

In this paper, the results of a photon-scattering experiment on ^{76}Se performed at the S-DALINAC facility at TU Darmstadt are presented. The experimental method allows for simultaneous study of the PDR, as well as certain $J = 1, 2$ MS and QOC states. The discussion of the results of this experiment are centered around possible candidates for these collective modes.

II. NUCLEAR RESONANCE FLUORESCENCE

Photon scattering, or nuclear resonance fluorescence (NRF), is a standard technique for probing nuclear dipole resonances extending below S_n such as the giant dipole and pygmy resonances. Photon beams used in NRF experiments are commonly produced by electron bremsstrahlung or laser Compton backscattering. Beams produced by bremsstrahlung, such as the ones used in this work, are mostly unpolarized and have an energy continuum spanning from low energy to an end-point energy E_0 corresponding to the initial electron energy. The discussion of experimental method and analysis will, consequently, focus on such conditions. A detailed overview of the bremsstrahlung photon-scattering method may be found in Ref. [45].

The resonant absorption of high-energy photons populating a bound state at energy E_x in the target nuclei is observed through subsequent γ decay to a lower-lying, possibly excited, state at energy E_f. Resonant absorption of photons in even-even nuclei directly excites primarily $J^\pi = 1^\pm, 2^+$ states. Angular intensity ratios of γ rays from elastic scattering (i.e., direct decay to the ground state after resonant absorption) in two detectors is sufficient for a spin assignment of excited states. The angular distribution of photons emitted through the spin sequence $J_0 \to J_x \to J_f$ at an angle θ with respect to the beam axis is given by the function $W_{J_0 \to J_x \to J_f}(\theta)$. For two observation points at $\theta = 90^\circ$ and $\theta = 130^\circ$ relative to an unpolarized beam of photons, the ratio $R_{90/130} = W(90^\circ)/W(130^\circ)$ is approximately 2.2 and 0.71 for the spin sequences $0 \to 2 \to 0$ and $0 \to 1 \to 0$, respectively.

The integrated scattering cross section for population of a state at energy E_f through direct excitation of a state at energy E_x through the (γ, γ') reaction may be extracted from the data as

$$I_f^S = \frac{A_{\gamma'}(\theta)}{N_T \Phi(E_x) \epsilon(E_{\gamma'}) W(\theta, \Delta\Omega)}, \tag{1}$$

where $A_{\gamma'}(\theta)$ is the measured peak area of the transition with energy $E_{\gamma'} = E_x - E_f$, $\epsilon(E_{\gamma'})$ is the absolute detector efficiency at E'_γ, N_T is the number of target nuclei, $\Phi(E_x)$ is the photon flux at energy E_x, and $W(\theta, \Delta\Omega)$ is the angular correlation function for the spin sequence with finite detector-angle corrections. The integrated cross section I_f^S is related to the decay width by

$$I_f^S = \int \sigma_f^S(E) dE = \pi^2 \left(\frac{\hbar c}{E_x}\right)^2 g \Gamma_0 \frac{\Gamma_f}{\Gamma}, \tag{2}$$

where $g = \frac{2J_x+1}{2J_0+1}$, Γ_0 denotes the ground-state transition width, and $\Gamma = \sum \Gamma_i$ is the total width of the directly excited state. Thus, observation of all decay branches allows one to deduce the state width and, using $\tau = \hbar/\Gamma$, its lifetime. Reduced

transition strengths may then be found using the relation

$$\Gamma_i = 8\pi \frac{2J_i+1}{2J_f+1} \sum_{\Pi L=1}^{\infty} \frac{(L+1)}{L[(2L+1)!!]^2} \times \left(\frac{E_\gamma}{\hbar c}\right)^{2L+1} B(\Pi L : J_i \to J_f) \uparrow, \quad (3)$$

which, for transitions of pure ΠL character, gives

$$\begin{aligned} \frac{B(E1)\uparrow}{[e^2\mathrm{fm}^2]} &= 2.866\times10^{-3}\frac{\Gamma_0}{[\mathrm{meV}]}\left(\frac{[\mathrm{MeV}]}{E_x}\right)^3 \\ \frac{B(M1)\uparrow}{[\mu_n^2]} &= 0.2592\frac{\Gamma_0}{[\mathrm{meV}]}\left(\frac{[\mathrm{MeV}]}{E_x}\right)^3 \\ \frac{B(E2)\uparrow}{[e^2\mathrm{fm}^4]} &= 6.225\times10^{3}\frac{\Gamma_0}{[\mathrm{meV}]}\left(\frac{[\mathrm{MeV}]}{E_x}\right)^5 \end{aligned} \quad (4)$$

for excitations from the 0^+ ground state in even-even nuclei.

III. EXPERIMENTAL DETAILS AND ANALYSIS

A photon-scattering experiment was performed on ^{76}Se at the Darmstadt High Intensity Photon Setup (DHIPS) at the Superconducting Darmstadt Linear Accelerator (S-DALINAC) facility, TU Darmstadt [46]. Monoenergetic electron beams from the injector of the superconducting linac are stopped in a copper radiator producing bremsstrahlung beams which are then collimated by copper (Fig. 1). The 4535.1-mg, 96.95% enriched sample of ^{76}Se at the first target station was irradiated by bremsstrahlung beams of end-point energies $E_0 = 5$, 7, and 9 MeV. The use of several end-point energies provides an excitation function (intensity of γ rays as a function of photon flux) and helps distinguish transitions from the exponentially increasing atomic background at low energies. Two BGO Compton-suppressed high-purity germanium (HPGe) detectors were positioned, one at $\theta = 90^\circ$ and one at $\theta = 130^\circ$, to maximize analyzing power for spin assignment of states. The ^{76}Se sample was sandwiched between two samples with total mass of either 1243.6 mg ^{27}Al ($E_0 = 5$ MeV and 7 MeV) or 634.2 mg ^{11}B ($E_0 = 9$ MeV) for the purpose of calibrating the product of efficiency and photon flux, $\Phi\epsilon(E)$, with the known cross sections. A sample calibration for $\Phi\epsilon(E)$ is shown in Fig. 2. The total irradiation time was 41 h, 77 h, and 121 h for the end-point energies 5, 7, and 9 MeV, respectively. A spectrum from one of the HPGe detectors is shown in Fig. 3.

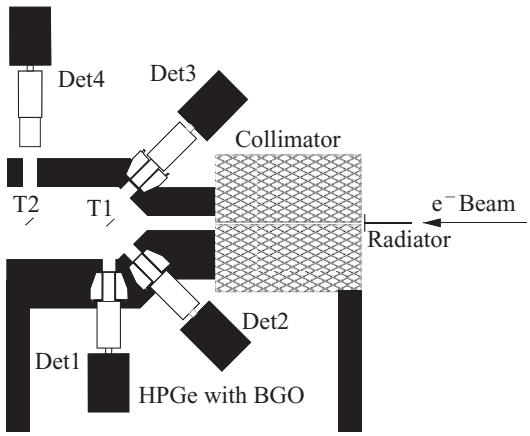

FIG. 1. Schematic of the experimental setup at the S-DALINAC facility [46]. Only the HPGe detectors "Det1" and "Det2" were used in the present work.

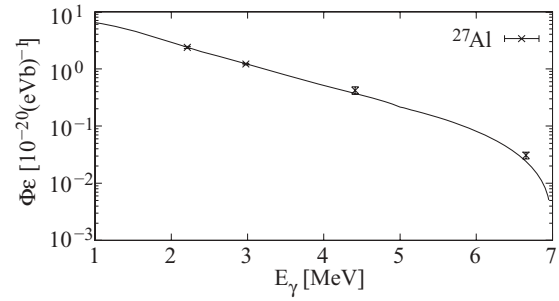

FIG. 2. Fit function of $\Phi\epsilon$ simulation data for the 130° detector for the $E_0 = 7$ MeV, scaled to the absolute value using transitions in ^{27}Al. Cross sections for transitions in ^{27}Al were obtained from Ref. [47].

The Monte Carlo code GEANT4 [48] was used to simulate detector efficiencies and the photon flux up to the end-point energy. The simulations were fit piecewise in intervals of 2 MeV starting at 1 MeV with polynomials of up to fourth order, which was sufficient to reproduce the mean in the interval with a reduced χ^2 near one. Data from ^{27}Al and ^{11}B were then used to scale $\Phi\epsilon(E)$ to its absolute value for each detector using a single scale parameter for all polynomials. Single and double escape peak subtraction was performed using ratios obtained from the efficiency simulation, which was checked with a ^{56}Co calibration source which also served as an energy calibration up to 3.6 MeV. At higher energies, known γ rays from ^{27}Al or ^{11}B were used for calibration.

Energy differences, angular distribution ratios, and the excitation function were used to determine the nature of the γ-ray transitions. For example, a decay from a directly populated $J = 1$ state to the 2_1^+ state is expected to have an angular

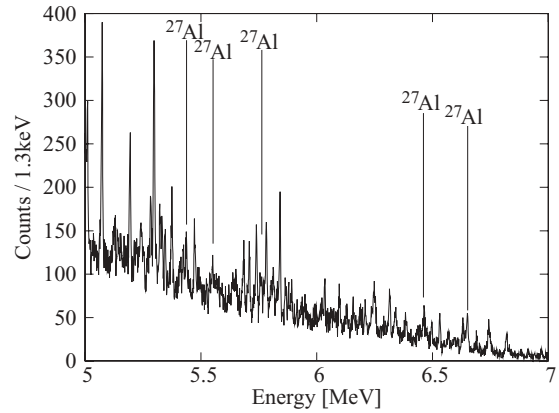

FIG. 3. Summed raw spectrum of the 90° detector from the 77-h run at $E_0 = 7$ MeV. The 5- to 7-MeV region shown contained most of the resolved dipole strength in ^{76}Se. The most intense transitions in the normalization standard ^{27}Al observed in this region have been marked.

distribution ratio between 0.85 and 0.97, and the observed intensity will be consistent with the beam photon flux at 559 keV above the transition energy, which may differ substantially from the photon flux at the transition energy. A calculation of the integrated cross section alone from data taken at two different end-point energies may give compelling evidence that a transition is to the 2_1^+ state. For example, the ratios of cross sections for the 4160.7-keV γ-ray $I(E_0 = 7\ \text{MeV})/I(E_0 = 9\ \text{MeV})$ and $I(E_0 = 5\ \text{MeV})/I(E_0 = 7\ \text{MeV})$ were found to be 0.68(15) and 0.53(9), respectively, assuming a dipole ground-state transition, while 0.67(13) and 1.1(2) are obtained assuming a dipole transition to the 2_1^+ state from the $J = 1$, 4720.0-keV state.

Fit peaks were considered if the peak area exceeded 2σ in both detectors; however, fit peaks not meeting this condition during a run of a particular end-point energy were considered (and often helpful in the analysis) when meeting the condition in at least one of the end-point-energy runs.

IV. RESULTS AND DISCUSSION

Inspection of evaluated data for ^{76}Se [49] suggests that several states observed in this work have been previously observed.

A $J = 1$ state at 2655.32 keV was previously observed [50] with a strong branch to the 2_1^+ state at 559.102 keV. In the present work, the transition to the 2_1^+ state was observed in the 7- and 9-MeV end-point runs but not the 5-MeV end-point run. A γ ray at nearly the same energy (2654.3 keV) was seen in all three runs; hence, we did not observe the literature state at 2655.32 keV in the 5-MeV run, but another transition was identified as the decay of a state at 3214 keV to the 2_1^+ state.

The state at 2950.6 keV had a previous assignment of $J^\pi = 1^+, 2^+$ [51], and the $R_{90/130} = 0.60(12)$ obtained in the present work leads to an assignment of 1^+. The state at 3604.3 keV was previously observed and assigned $J^\pi = 1^+, 2^+$ [52]. The angular anisotropy observed in the present work leads to an assignment of $J^\pi = 1^+$. The states at 4046.2 and 4971 keV may have been previously observed at energies 4044 and 4974(10) keV and were assigned $J^\pi = (1^+, 2^+, 3^+)$ which is reduced to $J^\pi = 1^{(+)}$ in the present work. A state at 5142.1 keV, assigned $J = 1$, was possibly observed at 5139.8(6) keV with an assignment of spin (1 to 4) in the data sheets [49].

Angular distribution ratios $R_{90/130}$ for the ground-state transitions of all identified states in this work are shown in Fig. 4 and are included in Table I. Transition properties given in Table I were evaluated from the data taken at the lowest E_0 in which the state could have been directly excited. A total of 87 previously unobserved states in ^{76}Se have been identified in this work. In addition, 26 decays to the 2_1^+ state, 2 decays to the 0_2^+ state, and 5 decays to the 2_2^+ state were also identified and were used in the determination of Γ of the respective excited states.

A. *E*1 strength distribution

The distribution of resolved dipole strength below 9 MeV is shown in Fig. 5, the vast majority of which are expected to be 1^- excitations. This expectation is generally justified by NRF studies of other nuclei in this energy range. However,

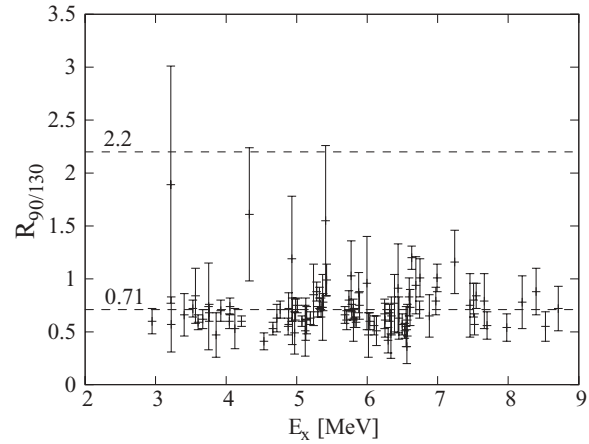

FIG. 4. Angular distribution ratios of intensity, $R_{90/130} = I(90^\circ)/I(130^\circ)$, of assigned ground-state transitions in ^{76}Se. An $R_{90/130}$ of 0.71 and 2.2 correspond to dipole and quadrupole ground-state tranisitons in even-even nuclei, respectively.

in particular it should be noted that at least some of the states around 3.9 MeV are suspected to be fragments of the scissors mode distribution, as discussed later. The average excitation strength appears to taper off around 7 MeV, which gives the distribution a resonance-like appearance. Structures such as this have often been suspected to be due to a neutron skin oscillation [6,7,53,54], which is theoretically predicted to occur in this energy region. The summed $B(E1)$ strength below 9 MeV amounts to 0.093(5) e^2 fm^2. According to the classical $E1$ sum rule [55]

$$\Sigma = 14.8\frac{NZ}{A}\text{MeV}e^2\text{fm}^2, \tag{5}$$

the observed strength exhausts 0.20(1)% of the sum, typical of studies of low-lying $E1$ strength. As will be discussed later in this section, these values should be viewed as lower limits of the $E1$ strength below 9 MeV.

The GDR is well known to be a source of significant $E1$ excitation strength in the energy region studied in this work. The centroid and width of the GDR are known to change as a function of A, and both experimental and theoretical studies of the GDR suggest that the centroid energy goes as $A^{-\delta}$ with $1/6 < \delta < 1/3$ [56]. Furthermore, the shape of the GDR is sensitive to the ground-state deformation of the nucleus. For a triaxially quadrupole-deformed nucleus the cross section of the GDR was recently expected to take the form [57]

$$\sigma \propto \sum_{n=1}^{3} \frac{E^2\Gamma^2}{\left(E^2 - E_n^2\right)^2 + E^2\Gamma^2}, \tag{6}$$

where

$$E_n = E_0 \exp\left[-\sqrt{\frac{5}{4\pi}}\beta_2 \cos\left(\gamma - \frac{2\pi n}{3}\right)\right]. \tag{7}$$

For the reasons stated above, precise knowledge of the $E1$ strength due to the GDR at low energy is highly desirable in order to facilitate an identification of an enhancement of strength due to any other source. However, the shape of the $E1$ strength function has been a topic of some debate over

TABLE I. Observed transitions of ^{76}Se. The reduced excitation strength from the ground state was calculated assuming the state has pure dipole character. Parities, when given, are from Ref. [49]. States for which the possibility of a $J = 2$ spin is not statistically excluded with 99% confidence are explicitly indicated. The uncertainties shown are statistical only.

E_x (keV)	J_x^π	J_f^π	E_γ (keV)	$R_{90/130}$	I_f^S (eV b)	$B(E1)\uparrow$ ($10^{-3}e^2$ fm^2)	$B(M1)\uparrow$ ($10^{-3}\mu_N^2$)	τ (fs)
2950.6(5)	1^+		2950.6(5)	0.60(12)	3.7(5)	0.46(5)	42(5)	109(19)
		2_1^+	2391.9(26)	0.27(47)	1.74(44)	0.081(27)	7.3(24)	
3214.4(4)	1,2		3216.7(8)	1.9(11)	0.73(25)	0.455(57)	41(5)	15.7(55)
		2_1^+	2654.3(5)	0.85(22)	5.2(7)	1.14(44)	103(40)	
3405.8(7)	1		3405.8(7)	0.66(20)	2.21(35)	0.161(26)	14.6(24)	296(47)
3528.6(3)	1		3528.6(3)	0.72(8)	8.39(78)	0.59(6)	53.4(54)	72.6(67)
3566.5(10)	1		3566.5(10)	0.84(26)	2.62(40)	0.18(3)	16.3(27)	227(34)
3604.3(3)	1^+		3604.3(3)	0.59(7)	7.3(7)	0.50(5)	45.2(45)	79.9(75)
3670.1(4)	1		3670.1(4)	0.62(9)	5.3(6)	0.36(4)	32.6(36)	106(11)
3752.0(14)	1		3752.0(14)	0.74(41)	2.1(6)	0.14(4)	12.7(36)	252(72)
3758.7(2)	1		3758.6(3)	0.68(8)	14.5(13)	2.0(1)	181(9)	8.59(86)
		2_1^+	3199.8(3)	1.23(17)	6.81(71)	0.30(4)	27.1(36)	
		0_2^+	2636.1(6)	0.42(14)	6.05(92)	2.41(46)	218(42)	
		2_2^+	2542.6(8)	2.09(92)	2.74(68)	0.24(7)	22(6)	
3857.7(11)	1		3857.7(11)	0.47(21)	2.07(43)	0.13(3)	11.8(27)	247(51)
3922.9(4)	1		3922.9(4)	0.70(10)	8.21(86)	0.52(6)	47(5)	60.1(63)
4046.2(3)	1		4046.2(3)	0.60(7)	10.34(97)	0.64(6)	58(5)	44.8(42)
4055.1(2)	1		4055.1(2)	0.74(8)	10.90(98)	0.67(6)	61(5)	42.3(38)
4125.4(10)	1		4125.4(10)	0.53(19)	2.31(43)	0.14(3)	13(3)	193(36)
4218.7(1)	1		4218.8(3)	0.60(5)	23.7(19)	2.87(16)	260(14)	4.27(37)
		2_1^+	3659.6(1)	0.96(7)	24.9(19)	0.92(11)	83(10)	
4329.2(4)	1,2		4329.7(6)	1.61(63)	2.4(5)	0.60(7)	54(6)	8.8(22)
		2_2^+	3112.4(6)	1.24(27)	8.1(11)	1.09(32)	99(29)	
4535.6(5)	1		4535.4(6)	0.41(8)	9.0(12)	0.83(9)	75(8)	14.6(25)
		2_1^+	3977.2(11)	0.70(26)	6.1(12)	0.16(5)	14.5(45)	
4662.9(3)	1		4662.7(3)	0.53(6)	25.9(25)	1.82(15)	165(14)	7.79(70)
		2_1^+	4104.2(5)	1.04(24)	8.2(11)	0.17(3)	15.4(27)	
4720.0(3)	1		4720.5(7)	0.63(13)	5.7(7)	0.77(6)	70(5)	9.2(13)
		2_1^+	4160.7(4)	0.78(11)	8.8(9)	0.35(6)	31.6(54)	
4766.8(3)	1		4766.8(3)	0.71(8)	13.3(11)	0.69(6)	62(5)	25.1(21)
4879.8(4)	1		4879.8(4)	0.55(8)	11.1(11)	0.57(6)	52(5)	28.7(28)
4886.9(6)	1		4886.9(6)	0.72(15)	8.2(10)	0.42(5)	38(5)	38.9(47)
4931.4(17)	1,2		4931.4(17)	1.19(59)	2.8(7)	0.14(4)	13(4)	114(30)
4938.4(15)	1		4938.4(15)	0.60(22)	5.0(9)	0.25(4)	23(4)	62(11)
4971.3(17)	$1^{(+)}$		4971.3(17)	0.49(20)	5.5(10)	0.28(5)	25(5)	55.5(96)
4984.7(3)	1		4984.3(4)	0.71(10)	11.8(11)	1.0(1)	90(9)	8.7(12)
		2_1^+	4426.1(5)	0.65(19)	8.6(14)	0.21(5)	19(5)	
5010.3(2)	1		5010.3(2)	0.75(7)	31.0(22)	2.09(14)	189(13)	5.27(50)
		2_1^+	4451.5(6)	0.62(18)	11.1(18)	0.21(5)	19(5)	
5073.9(1)	1		5073.7(1)	0.60(5)	46.2(30)	3.05(16)	276(14)	3.52(21)
		2_1^+	4515.8 (3)	0.94(11)	16.0(14)	0.30(3)	27(3)	
5122.0(2)	1		5122.0(2)	0.51(24)	5.8(13)	0.28(6)	25(5)	50(11)
5128.4(1)	1		5128.4(1)	0.62(20)	8.2(14)	0.40(7)	36(6)	35.4(60)
5142.1(7)	1		5142.1(7)	0.61(13)	7.6(9)	0.37(5)	33(5)	37.7(46)
5194.4(2)	1		5194.5(2)	0.63(6)	30.6(22)	2.45(13)	222(12)	3.28(25)
		2_1^+	4635.1(3)	0.68(7)	20.6(17)	0.47(6)	43(5)	
5239.4(8)	1		5239.7(12)	0.85(29)	12.2(22)	0.74(11)	67(10)	13.8(21)
		2_2^+	4023.1(10)	0.86(39)	3.4(7)	0.09(2)	8.1(18)	
5284.2(3)	1		5284.2(3)	0.88(9)	22.4(17)	1.05(8)	95(7)	12.14(93)
5298.4(1)	1		5298.4(1)	0.69(5)	66.6(42)	3.72(21)	336(19)	2.86(16)
		2_1^+	4739.6(5)	0.79(13)	10.1(11)	0.16(2)	14.5(18)	
		0_2^+	4175.0(12)	1.22(55)	2.6(6)	0.30(7)	27.1(63)	
5323.8(3)	1		5323.8(3)	0.82(10)	21.1(17)	0.99(8)	90(7)	12.7(10)

TABLE I. (*Continued.*)

E_x (keV)	J_x^π	J_f^π	E_γ (keV)	$R_{90/130}$	I_f^S (eV b)	$B(E1)\uparrow$ ($10^{-3}e^2$ fm^2)	$B(M1)\uparrow$ ($10^{-3}\mu_N^2$)	τ (fs)
5346.8(2)	1		5346.0(4)	0.73(9)	16.2(14)	1.37(9)	124(8)	4.97(52)
		2_1^+	4788.0(3)	0.67(17)	7.0(10)	0.17(3)	15.4(27)	
		2_2^+	4131.5(9)	0.74(22)	6.2(10)	0.23(5)	20.8(45)	
5367.3(13)	1		5367.3(13)	0.73(31)	4.1(9)	0.19(4)	17(4)	64(14)
5375.3(1)	1		5375.6(3)	0.78(8)	26.1(20)	2.67(15)	241(14)	2.07(19)
		2_1^+	4816.1(2)	0.97(9)	31.5(24)	0.89(11)	80(10)	
5411.2(3)	1,2		5412.4(14)	1.55(71)	5.6(14)	1.18(10)	107(9)	2.21(47)
		2_1^+	4852.0(3)	0.84(9)	20.0(17)	1.17(29)	106(26)	
5425.0(2)	1		5425.1(5)	0.99(15)	12.5(12)	1.15(8)	104(7)	5.18(58)
		2_1^+	4865.9(2)	0.91(14)	12.5(13)	0.32(5)	29(5)	
5685.3(3)	1		5685.3(3)	0.66(8)	20.5(18)	0.90(8)	81(7)	11.5(10)
5709.6(4)	1		5709.6(4)	0.61(9)	21.8(20)	0.95(9)	86(8)	10.65(98)
5740.5(3)	1		5740.5(3)	0.80(9)	28.4(23)	1.23(10)	111(9)	8.11(66)
5773.1(9)	1		5773.1(9)	1.03(33)	8.2(14)	0.36(6)	33(5)	27.7(46)
5783.3(3)	1		5783.3(3)	0.69(7)	40.3(30)	1.73(13)	156(12)	5.63(42)
5803.7(6)	1		5803.4(7)	0.61(20)	7.6(13)	0.84(11)	76(10)	4.5(11)
		2_1^+	5246.1(14)	1.03(39)	11.9(23)	0.35(12)	32(11)	
5813.7(5)	1		5813.7(5)	0.63(9)	19.5(19)	0.83(8)	75(7)	11.5(11)
5842.0(2)	1		5842.0(2)	0.59(5)	47.0(34)	2.00(14)	181(13)	4.73(34)
5879.4(6)	1		5879.4(6)	0.87(19)	10.3(13)	0.44(6)	40(5)	21.3(27)
5892.1(3)	1		5891.9(5)	0.75(13)	13.9(15)	1.06(9)	96(8)	4.83(65)
		2_1^+	5333.1(4)	1.36(33)	11.2(15)	0.23(5)	21(5)	
5997.2(4)	1,2		5998.4(14)	0.96(44)	4.7(11)	1.12(10)	101(9)	1.36(31)
		2_1^+	5438.0(4)	1.05 (13)	22.2(20)	1.42(37)	128(33)	
6035.4(4)	1		6035.4(4)	0.60(8)	23.6(22)	0.97(9)	88(8)	8.84(83)
6099.1(4)	1		6098.9(5)	0.56(9)	21.7(23)	1.35(11)	122(10)	4.04(43)
		2_1^+	5540.2(7)	1.12(25)	11.4(15)	0.19(3)	17(3)	
6131.2(6)	1		6131.2(6)	0.51(14)	12.1(19)	0.49(8)	44(7)	16.6(26)
6247.4(9)	1		6247.4(9)	0.67(14)	29.2(34)	1.16(14)	105(13)	6.67(79)
6254.0(9)	1		6254.0(9)	0.61(16)	24.4(32)	0.97(13)	88(12)	8.0(11)
6297.6(14)	1		6297.6(14)	0.42(12)	13.3(19)	0.53(8)	48(7)	14.4(21)
6315.6(3)	1		6315.6(3)	0.68(8)	44.3(37)	1.75(15)	158(14)	4.29(36)
6336.5(20)	1		6336.5(20)	0.48(23)	20.0(39)	0.78(15)	71(14)	9.5(19)
6342.3(11)	1		6342.3(11)	0.65(18)	25.8(39)	1.01(15)	91(14)	7.3(11)
6387.2(14)	1		6387.2(14)	0.77(27)	19.3(30)	0.75(12)	68(11)	9.6(15)
6437.8(19)	1		6437.8(19)	0.91(42)	15.2(35)	0.59(14)	53(13)	12.1(28)
6448.7(20)	1		6448.7(20)	0.63(20)	20.7(35)	0.80(14)	72(13)	8.8(15)
6497.4(6)	1		6497.4(6)	0.57(10)	24.8(28)	0.95(11)	86(10)	7.26(82)
6532.4(3)	1		6532.4(3)	0.51(7)	40.5(39)	1.54(15)	139(14)	4.39(42)
6550.7(13)	1		6550.7(13)	0.55(19)	11.2(20)	0.42(8)	38(7)	15.8(28)
6562.6(19)	1		6562.6(19)	0.36(16)	15.1(27)	0.57(10)	52(9)	11.7(21)
6570.1(9)	1		6570.1(9)	0.61(15)	25.3(34)	0.96(13)	87(12)	6.95(94)
6595.9(7)	1		6595.9(7)	0.83(18)	22.0(27)	0.83(10)	75(9)	7.9(10)
6608.2(8)	1		6608.2(8)	0.73(17)	19.9(27)	0.75(10)	68(9)	8.7(12)
6631.1(4)	1		6630.8(4)	1.20(11)	40.3(91)	2.3(4)	208(44)	2.0(4)
		2_1^+	6071.8(8)	0.85(19)	16.2(63)	0.24(11)	22(10)	
6691.2(8)	1		6691.2(8)	0.94(27)	11.5(19)	0.43(7)	39(6)	13.8(23)
6742.2(4)	1		6741.9(4)	0.71(8)	60.6(54)	2.89(27)	261(25)	1.6(2)
		2_1^+	6182.8(7)	0.76(16)	18.0(28)	0.22(5)	20(4)	
6748.7(5)	1		6748.4(5)	1.01(18)	38.4(68)	2.17(28)	196(33)	1.9(3)
		2_1^+	6190.0(6)	1.04(21)	19.8(50)	0.29(9)	26(8)	
6881.9(14)	1		6881.5(14)	0.65(20)	20.6(27)	1.40(24)	127(20)	2.2(4)
		2_1^+	6323.4(6)	1.48(39)	17.6(46)	0.31(12)	28(11)	
6973.0(8)	1		6973.0(8)	0.79(13)	26.7(27)	0.95(10)	86(9)	5.8(7)
6992.5(5)	1		6992.5(5)	1.01(13)	30.8(42)	1.10(15)	100(14)	4.7(7)

TABLE I. (*Continued.*)

E_x (keV)	J_x^π	J_f^π	E_γ (keV)	$R_{90/130}$	I_f^S (eV b)	$B(E1)\uparrow$ ($10^{-3}e^2$ fm^2)	$B(M1)\uparrow$ ($10^{-3}\mu_N^2$)	τ (fs)
7241.2(7)	1		7241.2(7)	1.16(30)	20.7(41)	0.71(14)	64(13)	6.2(12)
7457.6(7)	1		7457.6(7)	0.75(30)	18.7(40)	0.62(13)	56(12)	7.3(15)
7508.0(8)	1		7508.0(8)	0.80(16)	23.3(28)	0.77(9)	70(8)	5.8(7)
7521.7(7)	1		7521.3(7)	0.57(10)	32.2(55)	1.70(29)	154(26)	1.7(3)
		2_1^+	6963.9(13)	0.74(22)	18.4(43)	0.24(8)	22(8)	
7546.5(6)	1		7546.5(6)	0.84(12)	56.8(59)	1.87(19)	169(18)	2.3(2)
7658.3(12)	1		7658.3(12)	0.79(26)	13.9(23)	0.45(7)	41(7)	9.3(15)
7698.2(9)	1		7698.2(9)	0.56(13)	37.1(70)	1.20(23)	108(20)	3.2(4)
7978.5(8)	1		7978.5(8)	0.54(13)	25.2(61)	0.79(19)	71(17)	4.1(8)
8197.0(13)	1		8196.5(13)	0.78(25)	26.5(37)	1.55(27)	140(24)	1.1(2)
		2_2^+	6982.8(15)	0.91(28)	24.9(62)	0.47(18)	43(16)	
8394.4(10)	1		8394.4(10)	0.88(22)	29.8(42)	0.88(12)	80(11)	3.6(5)
8526.6(11)	1		8526.1(11)	0.55(14)	35.2(82)	2.20(36)	199(33)	0.7(1)
		2_1^+	7970.8(6)	0.93(22)	36(10)	0.54(20)	49(18)	
8709.4(13)	1		8709.4(13)	0.72(21)	41.7(64)	1.19(18)	108(17)	2.4(4)

the years, particularly at low energy (e.g., see Refs. [57–59]). Two $E1$ strength functions which are commonly used are the standard Lorentzian (SLO), which implies a cross section

$$\sigma^{\mathrm{SLO}} \propto \frac{E^2\Gamma^2}{\left(E^2 - E_0^2\right)^2 + E^2\Gamma^2} \tag{8}$$

and the generalized Lorentzian (GLO), based on the theory of Fermi liquids, resulting in

$$\sigma^{\mathrm{GLO}} \propto E\Gamma\left[\frac{E\Gamma(E)}{\left(E^2 - E_0^2\right)^2 + E^2[\Gamma(E)]^2}\right], \tag{9}$$

where $\Gamma(E) = \Gamma \times E^2/E_0^2$.

A global analysis of electric dipole strength data shows that extrapolation of the SLO generally overestimates strength at low γ-ray energies [60]. For this reason, in the recent work by Agvaanluvsan *et al.* [61], the GLO is used to extrapolate the $E1$ strength function in ^{117}Sn to low energy and find an enhancement of strength near 8 MeV. On the other hand, in recent work Tonchev *et al.* [12] extrapolate the SLO to low energy (4 MeV) in ^{138}Ba and find enhancements in strength above the SLO at about the same energy.

An experimental complication, pointed out by Rusev *et al.* [62] and supported by recent results from the HI$\vec{\gamma}$S facility [63], is that some of the apparent resonance structures in this energy region may partly be artifacts of increased branching to excited states with increasing excitation energy. These branches can be difficult to distinguish from the high background produced by Compton scattering and pair production in the target, as well as subsequent bremsstrahlung of the electrons and positrons. The increased branching to excited states at high energy is expected on a theoretical basis by considering the Brink hypothesis [64] along with the Lorentzian shape of the GDR. The inability to resolve these transitions would result in an underestimation of $E1$ strength at high energy. Compounding the problem is the high density of states as the excitation energy approaches the region where the nucleus is no longer bound: As the GDR strength becomes more fragmented, detectors with finite resolution may no longer be able to resolve individual states.

A double-SLO and double-GLO function were separately fitted to photoemission data of ^{76}Se and extrapolated to the region studied in the present work (Fig. 6). The SLO

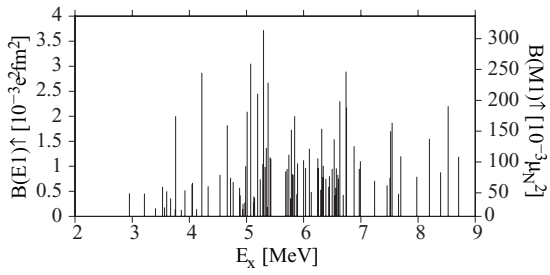

FIG. 5. Reduced excitation strength from the ground state to assigned $J = 1$ states. States with ambiguous spin listed in Table I appear under the assumption that $J = 1$.

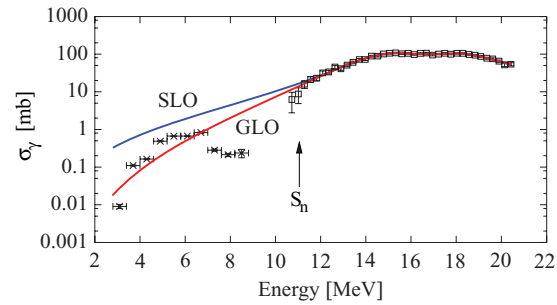

FIG. 6. (Color online) Photoexcitation cross section from the present work averaged over 600-keV intervals (crosses) and a previous (γ, n), (γ, pn), and $(\gamma, 2n)$ study (squares) [65]. The blue (red) curve corresponds to a double standard (generalized) Lorentzian fit to the photoemission data. The line width of each curve is approximately twice the statistical uncertainty of the fits, which is between 4.5% and 6.5% below S_n.

extrapolation overestimates the cross section in the energy range studied in this work. The GLO fit overestimates the cross section between 7 and 9 MeV, which could be an indication that considerable fragmentation of strength and unobserved branching may be present in this region. The GLO fit underestimates the cross section in the vicinity of 5 MeV, which could be an indication that there may be an additional source of $E1$ strength at this energy. Recent work on ^{78}Se [66] identified enhanced low-energy $E1$ strength around 8 MeV. In order to further test the $E1$ strength distribution in ^{76}Se, high-resolution experiments with monoenergetic photon beams have recently been performed at the HI$\vec{\gamma}$S facility and results will be published in a subsequent paper.

B. MS and QOC state candidates

With an $R_{4/2}$ of 2.38, ^{76}Se is expected to lie between the vibrational and axially symmetric rotational symmetry limits [corresponding to the U(5) and SU(3) limits in the IBM-2, respectively], and one would expect qualitative features of both limits to be present. The following discussion suggests that this expectation is met by properties of the presented MS candidates. A level scheme with transitions of interest is shown in Fig. 7 for reference.

To help identify the scissors mode, a semiempirical formula for the energy of the mode derived by Pietralla *et al.* [67] was used,

$$E(1^+_{\rm sc}) = 13.4\sqrt{1+(3\delta)^2}A^{-1/3}, \tag{10}$$

where [45]

$$\delta = \frac{3}{4}\sqrt{\frac{5}{\pi}}\beta_2 - \frac{15}{8\pi}\beta_2^2 + \frac{125}{32\pi^2}\beta_2^4 + \cdots . \tag{11}$$

With $\beta_2 = 0.309$ for ^{76}Se [68], Eqs. (10) and (11) predict the scissors mode to be at an excitation energy around 3.86 MeV.

A characteristic of the scissors mode in the vibrational limit is a strong $M1$ transition to the two-phonon symmetric 0^+_2 and 2^+_2 states. The $J = 1$ state observed at 3.759 MeV is very close to the energy prediction of the scissors mode. Assuming the observed decays from this state to the 0^+_2 and 2^+_2 states are purely $M1$, their summed strength is found to be a considerable 0.13 μ_N^2 for this decay channel. This agrees with

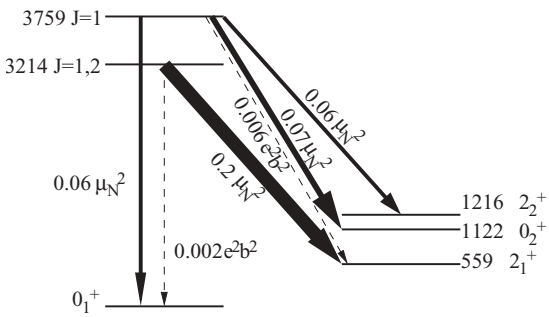

FIG. 7. Level scheme of mixed-symmetry candidates $1^+_{\rm sc}$ (3759 keV) and $2^+_{1,\rm ms}$ (3214 keV) with reduced transition strengths. Strengths are calculated from the data assuming pure $M1$ (solid lines) or pure $E2$ (dashed lines) multipolarities.

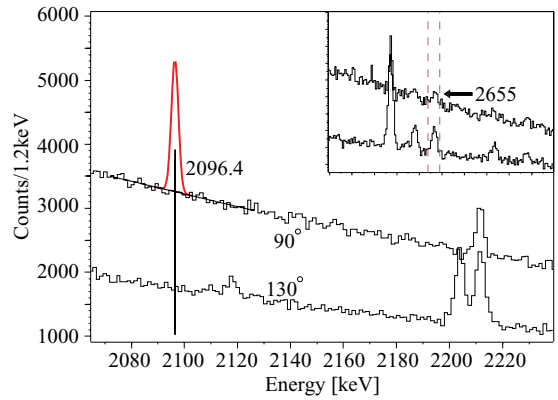

FIG. 8. (Color online) Raw spectra from the 5-MeV end-point energy run showing the expected peak form of the 2655.32 keV→ 2^+_1 transition using the branching ratio from Ref. [49]. The peak centered at 2654.3 keV (inset) was placed as a γ ray to the 2^+_1 state based on the excitation function.

the expectation of enhanced $M1$ transition strength between MS and FS two-phonon states. In addition, the transition to the ground state in the vibrational limit is forbidden, and the 0.06 μ_N^2 strength obtained in the present work supports a more vibrational rather than rotational structure (in well-deformed rotors, the ground-state transition strength is typically on the order of 1 μ_N^2). Other $J = 1$ states observed around this energy may be additional fragments of the scissors mode.

A candidate for the $2^+_{\rm MS,1}$ state has also been identified in this work. A strong transition of 2.654 MeV was identified as likely coming from the decay of a state at 3.214 MeV to the 2^+_1 state, as discussed above (Fig. 8). The characteristic strong decay to the 2^+_1 of 0.2 μ_N^2 (if assigned $M1$), its location of about $E(2^+_1)$ below the scissors mode candidate, and being the only 2^+ candidate in the region (see Fig. 4) make the state at 3.214 MeV the only $2^+_{\rm MS,1}$ candidate.

V. SUMMARY AND CONCLUSION

Photon-scattering experiments were performed on ^{76}Se at the S-DALINAC facility, TU Darmstadt, in order to study low-energy dipole strength in this nucleus and to provide further experimental data on the systematics of the PDR in the medium-mass region, which may also be used to challenge models used to calculate the $0\nu2\beta$-decay matrix element. The summed electric dipole strength was found to be 0.093(5) e^2 fm^2, exhausting 0.20(1)% of the classical $E1$ sum rule. This result represents a lower limit due to the expected contribution of inelastic decay width which cannot be determined from the present data. Candidates for low-lying mixed-symmetry states were presented. The $2^+_{1,\rm MS}$ candidate is interesting since this state has primarily been observed in weakly deformed nuclei. However, further experiments are needed to determine with certainty the parity of the dipole-excited states and the spin of the $2^+_{1,\rm MS}$ candidate. An enhancement in the photoabsorption cross section over a generalized Lorentzian extrapolation of photoemission data was observed near 5 MeV. It is likely that the data are incomplete due to unobserved strength, and further

study is needed for conclusive evidence of dipole strength enhancement at low energy.

ACKNOWLEDGMENTS

This work was supported by US DOE Grant No. DE-FG02-91ER40609, German DFG Grants No. SFB 634 and No. Pi393/2-1, and US NSF Grant No. PHY-0956310. V. Werner acknowledges support by HIC for FAIR within the LOEWE program by the state of Hesse. D. Savran acknowledges support by the Helmholtz Alliance Program of the Helmholtz Association (HA216/EMMI). The authors thank G. Rusev, A. Tonchev, F. Iachello, M. Scheck, and B. P. Crider for discussions.

[1] R.-D. Herzberg, P. von Brentano, J. Eberth, J. Enders, R. Fischer, N. Huxel, T. Klemme, P. von Neumann-Cosel, N. Nicolay, N. Pietralla *et al.*, Phys. Lett. B **390**, 49 (1997).
[2] R.-D. Herzberg, C. Fransen, P. von Brentano, J. Eberth, J. Enders, A. Fitzler, L. Käubler, H. Kaiser, P. von Neumann-Cosel, N. Pietralla *et al.*, Phys. Rev. C **60**, 051307 (1999).
[3] N. Pietralla, Z. Berant, V. N. Litvinenko, S. Hartman, F. F. Mikhailov, I. V. Pinayev, G. Swift, M. W. Ahmed, J. H. Kelley, S. O. Nelson *et al.*, Phys. Rev. Lett. **88**, 012502 (2001).
[4] J. Endres, E. Litvinova, D. Savran, P. A. Butler, M. N. Harakeh, S. Harissopulos, R.-D. Herzberg, R. Krücken, A. Lagoyannis, N. Pietralla *et al.*, Phys. Rev. Lett. **105**, 212503 (2010).
[5] T. Hartmann, M. Babilon, S. Kamerdzhiev, E. Litvinova, D. Savran, S. Volz, and A. Zilges, Phys. Rev. Lett. **93**, 192501 (2004).
[6] S. Volz, N. Tsoneva, M. Babilon, M. Elvers, J. Hasper, R.-D. Herzberg, H. Lenske, K. Lindenberg, D. Savran, and A. Zilges, Nucl. Phys. A **779**, 1 (2006).
[7] D. Savran, M. Elvers, J. Endres, M. Fritzsche, B. Löher, N. Pietralla, V. Y. Ponomarev, C. Romig, L. Schnorrenberger, K. Sonnabend *et al.*, Phys. Rev. C **84**, 024326 (2011).
[8] R. Schwengner, G. Rusev, N. Benouaret, R. Beyer, M. Erhard, E. Grosse, A. R. Junghans, J. Klug, K. Kosev, L. Kostov *et al.*, Phys. Rev. C **76**, 034321 (2007).
[9] N. Benouaret, R. Schwengner, G. Rusev, F. Dönau, R. Beyer, M. Erhard, E. Grosse, A. R. Junghans, K. Kosev, C. Nair *et al.*, Phys. Rev. C **79**, 014303 (2009).
[10] R. Schwengner, G. Rusev, N. Tsoneva, N. Benouaret, R. Beyer, M. Erhard, E. Grosse, A. R. Junghans, J. Klug, K. Kosev *et al.*, Phys. Rev. C **78**, 064314 (2008).
[11] A. Makinaga, R. Schwengner, G. Rusev, F. Dönau, S. Frauendorf, D. Bemmerer, R. Beyer, P. Crespo, M. Erhard, A. R. Junghans *et al.*, Phys. Rev. C **82**, 024314 (2010).
[12] A. P. Tonchev, S. L. Hammond, J. H. Kelley, E. Kwan, H. Lenske, G. Rusev, W. Tornow, and N. Tsoneva, Phys. Rev. Lett. **104**, 072501 (2010).
[13] R. Mohan, M. Danos, and L. C. Biedenharn, Phys. Rev. C **3**, 1740 (1971).
[14] Y. Suzuki, K. Ikeda, and H. Sato, Prog. Theor. Phys. **83**, 180 (1990).
[15] P. Van Isacker, M. A. Nagarajan, and D. D. Warner, Phys. Rev. C **45**, R13 (1992).
[16] T. Kobayashi, O. Yamakawa, K. Omata, K. Sugimoto, T. Shimoda, N. Takahashi, and I. Tanihata, Phys. Rev. Lett. **60**, 2599 (1988).
[17] P. Adrich, A. Klimkiewicz, M. Fallot, K. Boretzky, T. Aumann, D. Cortina-Gil, U. D. Pramanik, T. W. Elze, H. Emling, H. Geissel *et al.* (LAND-FRS Collaboration), Phys. Rev. Lett. **95**, 132501 (2005).
[18] O. Wieland, A. Bracco, F. Camera, G. Benzoni, N. Blasi, S. Brambilla, F. C. L. Crespi, S. Leoni, B. Million, R. Nicolini *et al.*, Phys. Rev. Lett. **102**, 092502 (2009).
[19] F. Iachello, Phys. Lett. B **160**, 1 (1985).
[20] E. Majorana, Nuovo Cimento **14**, 171 (1937).
[21] G. Racah, Nuovo Cimento **14**, 322 (1937).
[22] H. Klapdor-Kleingrothaus, I. Krivosheina, A. Dietz, and O. Chkvorets, Phys. Lett. B **586**, 198 (2004).
[23] C. A. Ur and the GERDA collaboration, Nucl. Phys. B, Proc. Suppl. **217**, 38 (2011).
[24] C. E. Aalseth, E. Aguayo, M. Amman, F. Avignone III, H. Back, X. Bai, A. Barabash, P. Barbeau, M. Bergevin, F. Bertrand *et al.*, Nucl. Phys. B, Proc. Suppl. **217**, 44 (2011).
[25] E. Caurier, J. Menéndez, F. Nowacki, and A. Poves, Phys. Rev. Lett. **100**, 052503 (2008).
[26] F. Šimkovic, A. Faessler, V. Rodin, P. Vogel, and J. Engel, Phys. Rev. C **77**, 045503 (2008).
[27] J. Barea and F. Iachello, Phys. Rev. C **79**, 044301 (2009).
[28] J. Kotila and F. Iachello, Phys. Rev. C **85**, 034316 (2012).
[29] M. Babilon, N. V. Zamfir, D. Kusnezov, E. A. McCutchan, and A. Zilges, Phys. Rev. C **72**, 064302 (2005).
[30] N. A. Smirnova, N. Pietralla, T. Mizusaki, and P. V. Isacker, Nucl. Phys. A **678**, 235 (2000).
[31] W. Andrejtscheff, C. Kohstall, P. von Brentano, C. Fransen, U. Kneissl, N. Pietralla, and H. Pitz, Phys. Lett. B **506**, 239 (2001).
[32] A. Faessler, Nucl. Phys. **85**, 653 (1966).
[33] F. Iachello, Phys. Rev. Lett. **53**, 1427 (1984).
[34] N. Pietralla, C. Fransen, D. Belic, P. von Brentano, C. Frießner, U. Kneissl, A. Linnemann, A. Nord, H. H. Pitz, T. Otsuka *et al.*, Phys. Rev. Lett. **83**, 1303 (1999).
[35] N. Pietralla, C. Fransen, P. von Brentano, A. Dewald, A. Fitzler, C. Frießner, and J. Gableske, Phys. Rev. Lett. **84**, 3775 (2000).
[36] F. Iachello and A. Arima, *The Interacting Boson Model* (Cambridge University Press, Cambridge, UK, 1987).
[37] T. Otsuka, A. Arima, and F. Iachello, Nucl. Phys. A **309**, 1 (1978).
[38] N. Pietralla, P. von Brentano, and A. Lisetskiy, Prog. Part. Nucl. Phys. **60**, 225 (2008).
[39] N. Lo Iudice and F. Palumbo, Phys. Rev. Lett. **41**, 1532 (1978).
[40] D. Bohle, A. Richter, W. Steffen, A. Dieperink, N. L. Iudice, F. Palumbo, and O. Scholten, Phys. Lett. B **137**, 27 (1984).
[41] A. Richter, Prog. Part. Nucl. Phys. **34**, 261 (1995).
[42] T. C. Li, N. Pietralla, C. Fransen, H. v. Garrel, U. Kneissl, C. Kohstall, A. Linnemann, H. H. Pitz, G. Rainovski, A. Richter *et al.*, Phys. Rev. C **71**, 044318 (2005).
[43] N. Pietralla, P. von Brentano, R.-D. Herzberg, U. Kneissl, J. Margraf, H. Maser, H. H. Pitz, and A. Zilges, Phys. Rev. C **52**, R2317 (1995).
[44] J. Enders, P. von Neumann-Cosel, C. Rangacharyulu, and A. Richter, Phys. Rev. C **71**, 014306 (2005).
[45] U. Kneissl, H. Pitz, and A. Zilges, Prog. Part. Nucl. Phys. **37**, 349 (1996).
[46] K. Sonnabend, D. Savran, J. Beller, M. Bssing, A. Constantinescu, M. Elvers, J. Endres, M. Fritzsche, J. Glorius, J. Hasper *et al.*, Nucl. Instrum. Methods A **640**, 6 (2011).

[47] R. Vodhanel, R. Moreh, W. C. Sellyey, M. K. Brussel, and B. H. Wildenthal, Phys. Rev. C **35**, 921 (1987).
[48] S. Agostinelli, J. Allison, K. Amako, J. Apostolakis, H. Araujo, P. Arce, M. Asai, D. Axen, S. Banerjee, G. Barrand *et al.*, Nucl. Instrum. Methods A **506**, 250 (2003).
[49] B. Singh, Nucl. Data Sheets **74**, 63 (1995).
[50] C. B. Zamboni and R. N. Saxena, Phys. Rev. C **39**, 2379 (1989).
[51] B. S. Dzhelepov, A. G. Dmitriev, Z. Zhelev, N. N. Zhukovskii, L. N. Moskvin, and V. I. Fominykh, Izv. Akad. Nauk SSSR, Ser. Fiz. **34**, 2062 (1970).
[52] D. Ardouin, R. Tamisier, M. Vergnes, G. Rotbard, J. Kalifa, G. Berrier, and B. Grammaticos, Phys. Rev. C **12**, 1745 (1975).
[53] T. Hartmann, J. Enders, P. Mohr, K. Vogt, S. Volz, and A. Zilges, Phys. Rev. C **65**, 034301 (2002).
[54] D. Savran, M. Fritzsche, J. Hasper, K. Lindenberg, S. Müller, V. Y. Ponomarev, K. Sonnabend, and A. Zilges, Phys. Rev. Lett. **100**, 232501 (2008).
[55] A. Bohr and B. R. Mottelson, *Nuclear Structure* (Benjamin, Reading, MA, 1975).
[56] J. Speth and A. van der Woude, Rep. Prog. Phys. **44**, 719 (1981).
[57] A. Junghans, G. Rusev, R. Schwengner, A. Wagner, and E. Grosse, Phys. Lett. B **670**, 200 (2008).
[58] E. Běták, J. Kopecky, and F. Cvelbar, Phys. Rev. C **46**, 945 (1992).
[59] B. Bush and Y. Alhassid, Nucl. Phys. A **531**, 27 (1991).
[60] C. M. McCullagh, M. L. Stelts, and R. E. Chrien, Phys. Rev. C **23**, 1394 (1981).
[61] U. Agvaanluvsan, A. C. Larsen, R. Chankova, M. Guttormsen, G. E. Mitchell, A. Schiller, S. Siem, and A. Voinov, Phys. Rev. Lett. **102**, 162504 (2009).
[62] G. Rusev, R. Schwengner, R. Beyer, M. Erhard, E. Grosse, A. R. Junghans, K. Kosev, C. Nair, K. D. Schilling, A. Wagner *et al.*, Phys. Rev. C **79**, 061302 (2009).
[63] G. Rusev (private communication, 2011).
[64] D. M. Brink, Ph.D. thesis, Oxford University, 1955.
[65] P. Carlos, H. Beil, R. Bergre, J. Fagot, A. Leprtre, A. Veyssire, and G. Solodukhov, Nucl. Phys. A **258**, 365 (1976).
[66] G. Schramm, R. Massarczyk, A. R. Junghans, T. Belgya, R. Beyer, E. Birgersson, E. Grosse, M. Kempe, Z. Kis, K. Kosev *et al.*, Phys. Rev. C **85**, 014311 (2012).
[67] N. Pietralla, P. von Brentano, R.-D. Herzberg, U. Kneissl, N. Lo Iudice, H. Maser, H. H. Pitz, and A. Zilges, Phys. Rev. C **58**, 184 (1998).
[68] S. Raman, C. W. Nestor, Jr., and P. Tikkanen, At. Data Nucl. Data Tables **78**, 1 (2001).